AIP | Applied Physics Letters

Effect of free electrons on nanoparticle charging in a negative direct current corona charger

A. Aliat, C.-J. Tsai, C.-T. Hung, and J.-S. Wu

Citation: Applied Physics Letters **93**, 154103 (2008); doi: 10.1063/1.2967470
View online: http://dx.doi.org/10.1063/1.2967470
View Table of Contents: http://scitation.aip.org/content/aip/journal/apl/93/15?ver=pdfcov
Published by the AIP Publishing

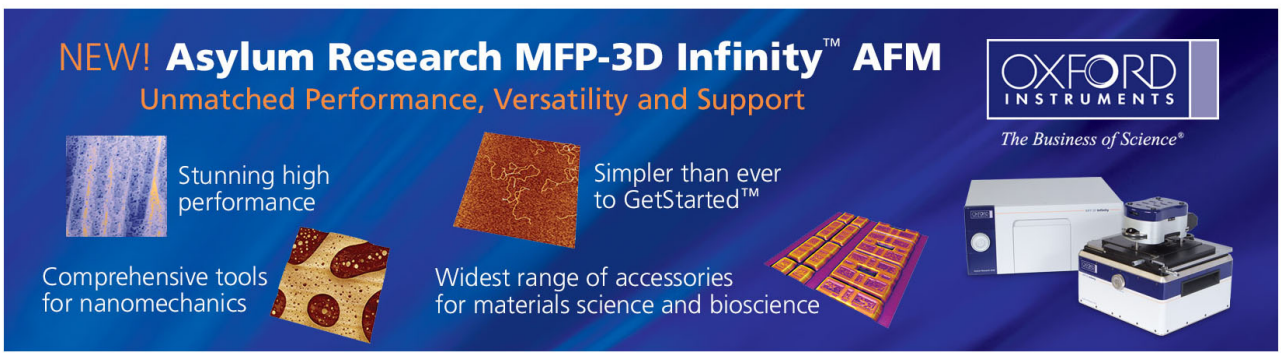

Effect of free electrons on nanoparticle charging in a negative direct current corona charger

A. Aliat,[1,2] C.-J. Tsai,[2] C.-T. Hung,[1] and J.-S. Wu[1,a)]
[1]*Department of Mechanical Engineering, National Chiao Tung University, Hsinchu 30050, Taiwan*
[2]*Institute of Environmental Engineering, National Chiao Tung University, Hsinchu 30050, Taiwan*

(Received 17 May 2008; accepted 14 July 2008; published online 16 October 2008)

A two-dimensional numerical model is proposed in this letter to take into account the effects of free electrons on nanoparticle charging in a negative direct current wire-tube corona charger. Numerical results are in excellent agreement with the experimental data by using a capturing probability of electrons onto nanoparticles with a value of 0.013. These free electrons contribute greatly to the charging efficiency at high products of mean ion concentration and mean residence time, which explains very well the large discrepancy found in earlier models that considered only negative ions. © *2008 American Institute of Physics*. [DOI: 10.1063/1.2967470]

Nanoparticle charging becomes increasingly important in aerosol science with numerous applications including aerosol instrumentation, ultrafine particle control, and material synthesis.[1] Several unipolar chargers[2,3] have been constructed to create charged particles, and a theoretically correct model is crucial to optimally design their charging efficiency. However, the high negative charging efficiency of nanoparticles found at high charging intensities, where the Nt product (mean ion concentration N and mean residence time t) is larger than 10^7 s cm^{-3}, remains a physical phenomenon that is still poorly understood. Indeed, with this condition the measured average charges carried by nanoparticles (diameter of 65 nm, concentration of 10^5 cm^{-3}) by Marquard *et al.*[2] within a negative direct current (dc) corona charger were found to be much higher than those expected with the largely utilized diffusion theory that applies Fuchs's model.[4,5] The latter had been applied to predict accurately a positive charging process[2] and thus led us to suspect that free electrons might play an important role in the mechanism of high negative charging. Previous modeling ignored the contribution from electrons simply because of their low concentration in a typical negative dc corona charger, although the attachment coefficient of electrons is known to be much higher than that of ions.[6] Recently, Marquard *et al.*[7] also speculated that electrons might play an important role although they did not provide any solid theoretical/numerical evidence. Moreover, previous charging modelings only considered the one-dimensional case, which necessitates averaged values on the electric field and ion concentration distributions that may lead to inaccuracy in the numerical results. This also excluded the understanding of the detailed path of nanoparticles within the charger device.

In this letter, we propose a two-dimensional (2D) charging model by taking into account free electrons within a negative dc wire-tube corona charger. This model considers (1) the corona discharge model and (2) the nanoparticle charging model. Numerical results are then compared to the experimental data obtained by Marquard *et al.*[2] and discussed.

The electrostatic precipitator charger device utilized by Marquard *et al.*[2] is a stainless steel tube of length $L=26$ cm with a wire at the center with dry air flowing at atmospheric pressure. The inner wire of radius $r_w=0.05$ mm is subjected to a negative dc voltage φ_w with a current intensity I (per unit length), whereas the outer electrode of radius $R=2$ cm is grounded. The corona discharge is assumed to be axisymmetric and invariant in the axial direction. Time-independent continuity equations of electrons and positive and negative ions are as follows:[8]

$$\frac{1}{r}\frac{d}{dr}(rN_e\mu_eE) = (\alpha - \eta)N_e\mu_eE, \tag{1}$$

$$-\frac{1}{r}\frac{d}{dr}(rN_p\mu_pE) = \alpha\ N_e\mu_eE, \tag{2}$$

$$\frac{1}{r}\frac{d}{dr}(rN_n\mu_nE) = \eta\ N_e\mu_eE, \tag{3}$$

where r is the radial coordinate, and N_e, N_p, and N_n are the number densities of electrons and positive and negative air ions, respectively. The mobility of air ions is assumed to be constant and is given in Ref. 2, while those of electrons (μ_e), ionization coefficient (α), and the attachment coefficient (η) depending on the local electric field are given in Ref. 9. Boundary conditions for air ions are $N_n(r_w)=0$ and $N_p(R)=0$ because of repulsion from the electrodes, while that of electrons is given on the wire's surface from the current intensity determined experimentally:[8,10] $I=2\pi\ r_we\Sigma_i\mu_iN_iE$. Diffusion of ions and electrons is not considered and the ambient temperature is assumed to be uniform within the charger.

Expression of the electric field is obtained from the Gauss equation in the low-field region where the negative ions are dominant and by considering the onset electric field strength E_w on the wire's surface provided by Peek's law.[11] It is then expressed as

$$E(r) = \left[\left(\frac{I}{\varepsilon_0 2\pi\mu_n}\right)\left(1 - \frac{r_w^2}{r^2}\right) + \left(\frac{E_wr_w}{r}\right)^2\right]^{1/2}, \tag{4}$$

where ε_0 is the vacuum dielectric constant. In this study, we assume that the electric field is only influenced by air ions because they mainly cause the space charge since the concentration of air ions ($\sim 10^{10}$ cm^3) is much larger than that

a)Electronic mail: chongsin@faculty.nctu.edu.tw.

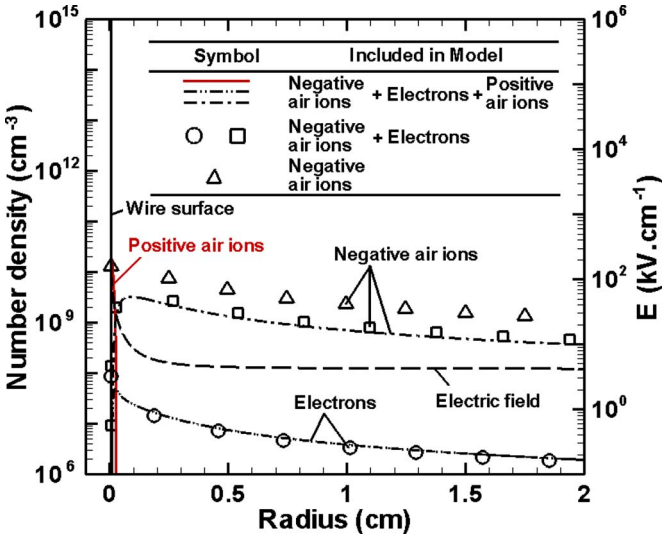

FIG. 1. (Color online) Distribution of electric field, electrons, and positive and negative ions ($\varphi_w=-9.5$ kV and $I=19.2$ μA cm^{-1}). The wire-tube corona charger is 2 cm in radius submitted at $\varphi_w=-9.5$ kV and $I=19.2$ μA cm^{-1}.

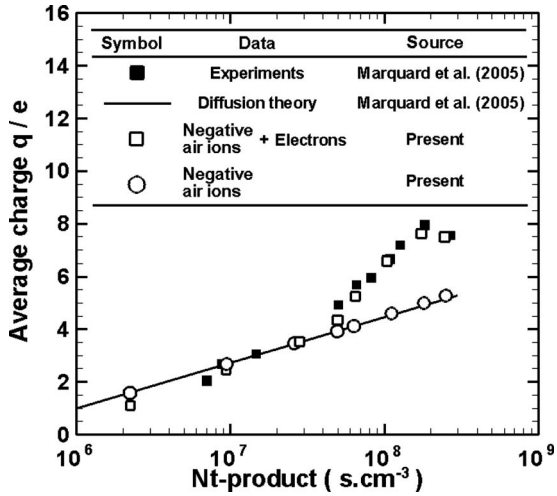

FIG. 2. Average charge carried by nanoparticles with diameter of 65 nm as a function of the *Nt* product. The wire-tube corona charger is 2 cm in radius and 26 cm in length. Mean air flow speed in the tube is 2 m s^{-1}.

of nanoparticles ($\sim 10^5$ cm^{-3}) and electrons (approximately two orders of magnitude smaller than that of ions).

Figure 1 shows the distribution of electric field [Eq. (4)], electrons, and positive and negative ions [solving Eqs. (1)–(3)] with $\varphi_w=-9.5$ kV and $I=19.2$ μA cm^{-1}. The electron concentration is about two orders of magnitude smaller than that of the negative ions in the low-field region, which further justifies the use of Eq. (4). Although the existence of the positive ions in the very vicinity of the wire (<0.03 cm) does induce a small error in the electric field by using Eq. (4), it can be used to predict the electric field across the gap, as shown in Ref. 10. In addition, Fig. 1 shows that essentially the same data for the distributions of electrons and negative ions are obtained whether the positive ions are considered or not. Note that by considering only negative ions [Eq. (3)] as diffusion theory does, the concentration of negative ions becomes much higher because they transport the corona current entirely. The electric field decreases rapidly but becomes nearly constant after ~ 0.4 cm from the wire's surface.

The distribution of nanoparticles is assumed to be axisymmetric and is governed by the following 2D time-independent continuity equations:

$$U_z\frac{\partial Y_{d,q}}{\partial z}+\mu_{d,q}E\frac{\partial Y_{d,q}}{\partial r}+\mu_{d,q}Y_{d,q}\left(\frac{E}{r}+\frac{\partial E}{\partial r}\right)-D_d\left(\frac{1}{r}\frac{\partial Y_{d,q}}{\partial r}+\frac{\partial^2 Y_{d,q}}{\partial r^2}+\frac{\partial^2 Y_{d,q}}{\partial z^2}\right)=-\beta^n_{d,q}N_nY_{d,q}-\beta^e_{d,q}N_eY_{d,q}+\beta^n_{d,q+1}N_nY_{d,q+1}+\beta^e_{d,q+1}N_eY_{d,q+1}, \quad (5)$$

where the axial air gas carrier's velocity U_z is described by a fully developed turbulent pipe flow profile.[12] $Y_{d,q}$, $\mu_{d,q}$, and D_d are the number fraction, the mobility, and the diffusion coefficients related to the spherical nanoparticles of diameter d with charge q, respectively. Terms $\beta^n_{d,q}$ and $\beta^e_{d,q}$ are attachment coefficients of negative ions and electrons to nanoparticles, respectively, and are both given by Fuchs's model:[4,5]

$$\beta^i_{d,q}=\pi\theta_i\gamma_i\bar{c}_i\delta_i^2\exp\left[-\frac{\Phi(\delta_i)}{kT_i}\right]\times\left\{1+\exp\left[-\frac{\Phi(\delta_i)}{kT_i}\right]\frac{\theta_i\gamma_i\bar{c}_i\delta_i^2}{2dD_i}\times\int_0^{d/2\delta_i}dy\exp\left[\frac{\Phi(d/2y)}{kT_i}\right]\right\}^{-1}, \quad (6)$$

where the subscript i denotes either electron or negative ions. Detailed descriptions of the above various parameters can be found in Refs. 5 and 13 and are thus skipped here for brevity. Among these, δ_i is the limiting-sphere radius in which the ions or electrons can be captured; γ_i is the probability of capture when the electrons/ions approach the nanoparticle within a distance of δ_i.[14] The ionic probability of capture is usually set as $\gamma_n=1$, while that of electrons (γ_e) will be discussed later. Boundary conditions at the entrance of the discharge tube are $Y_{d,q=0}(z=0)=1$ and $Y_{d,q\neq 0}(z=0)=0$, whereas $\partial Y_{d,q}/\partial\vec{n}=0$ ($\vec{n}$ is the normal unit vector on the considered surface) is applied at the exit of the tube, wire, and grounded electrode. All equations in this letter are discretized by the central finite-difference method and solved using the iterative algorithm for matrix equations.

Figure 2 illustrates the predicted average charge with the same experimental conditions of Marquard *et al.*[2] as a function of the *Nt* product. When only negative ions are considered in Eq. (5), we can reproduce the prediction using the diffusion theory by Marquard *et al.*,[2] but we cannot reproduce the experimental data as $Nt\geq 5\times 10^7$ s cm^{-3}. In addition, a relatively large discrepancy is also found in low *Nt* products. As both negative ions and electrons are considered in Eq. (5), the current model can faithfully reproduce the experimental average charge at all ranges of the *Nt* product with a fitted probability of capture $\gamma_e=0.013$, which is possibly caused by the high velocity of electrons ($v_e=\mu_eE$). Indeed, the electrons are then more difficult capture but reach the limiting-sphere's surface of nanoparticles with a much greater flux ($=N_ev_e$). Note that Romay[13] also found a lower probability than unity ($\gamma_e=0.4$) in the case of helium gas carrier for a lower electric field mean value ($E\sim 100$ V cm^{-1}). At low *Nt* products, the predicted values

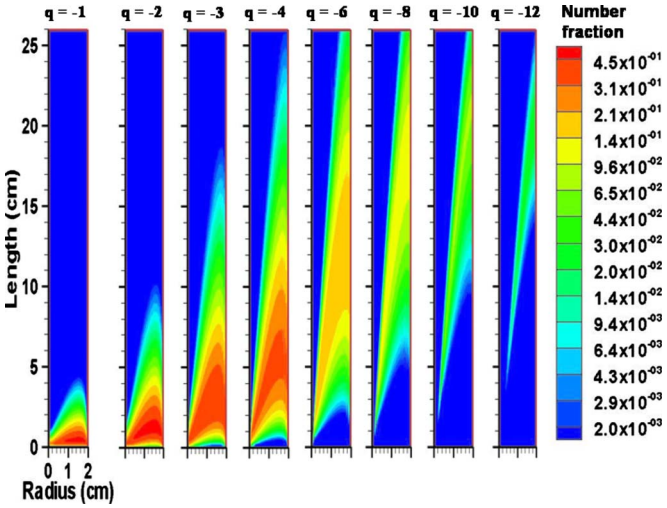

FIG. 3. (Color online) Distribution of negatively charged nanoparticles with diameter of 65 nm and charges $q=-1,-2,-3,-4,-6,-8,-10,-12$. The wire-tube corona charger is 2 cm in radius and 26 cm in length with $\varphi_w=-9.5$ kV and $I=19.2$ μA cm^{-1}. Mean air flow speed in the tube is 2 m s^{-1}.

are lower than those of the diffusion theory because the current is actually carried by both electrons and negative air ions. However, the electron concentration is too low to contribute to the charging process in this case. At high Nt products, the concentration of electrons is lower compared to that of the ions but high enough to contribute appreciably to the charging process. Interestingly, the average charge observed both experimentally and numerically starts to drop for $Nt \geq 2\times10^8$ s cm^{-3}, which can be well explained in Fig. 3. Figure 3 illustrates the path of nanoparticles with charges $q=-1,-2,-3,-4,-6,-8,-10,-12$ at $Nt\sim2\times10^8$ s cm^{-3}. Clearly, most nanoparticles exit the charger with $-12\leq q\leq -6$, which results in the very high average charge observed experimentally. As charging intensity increases, more particles are charged inside the tube in the early portion of the tube and move faster to the grounded electrode in the later portion due to the increasing amount of charges on them and the stronger electric field. If too many highly charged particles moved to the outer grounded electrode, then the average charge at the exit may eventually decrease.

In conclusion, the 2D charging model presented in this letter shows that it is necessary to take into account the effect of free electrons on the negative nanoparticle charging process. Numerical results are in very good agreement with those observed experimentally should the probability of capture for electrons γ_e be set as 0.013 for nanoparticles with 65 nm diameter. More measurements using different sizes of nanoparticles are strongly recommended to further test the validity of the charging model developed in the present study.

The financial support of the National Science Council of Taiwan through Contract Nos. NSC-96-2628-E-009-008-MY3, NSC-96-2120-M-006-005, and NSC-96-2628-E-009-134-MY3 is gratefully acknowledged.

[1]S. K. Friedlander and D. Y. H. Pui, NSF Workshop report, 2003.
[2]A. Marquard, M. Kasper, J. Meyer, and G. Kasper, J. Electrost. **63**, 693 (2005).
[3]D. R. Chen and D. Y. H. Pui, J. Nanopart. Res. **1**, 115 (1999).
[4]N. A. Fuchs, Geofis. Pura Appl. **56**, 185 (1963).
[5]J. Jiang, M. H. Lee, and P. Biswas, J. Electrost. **65**, 209 (2007).
[6]F. J. Romay and D. Y. H. Pui, J. Aerosol Sci. **23**, 679 (1992).
[7]A. Marquard, J. Meyer, and G. Kasper, Aerosol Sci. Technol. **41**, 611 (2007).
[8]K. Yanallah, S. Hadj Ziane, A. Belasri, and Y. Meslem, J. Mol. Struct. **777**, 125 (2006).
[9]M. Abdel-Salam, M. Nakano, and A. Mizuno, J. Phys. D **40**, 1919 (2007).
[10]F. Pontiga, C. Soria, A. Castellanos, and J. D. Skalny, Ozone: Sci. Eng. **24**, 447 (2002).
[11]F. W. Peek, *Dielectric Phenomena in High-Voltage Engineering* (McGraw-Hill, New York, 1929).
[12]E.-S. Zanoun, F. Durst, O. Bayoumy, and A. Al-Salaymeh, Exp. Therm. Fluid Sci. **32**, 249 (2007).
[13]F. J. Romay, Ph.D. thesis, University of Minnesota, 1992.
[14]M. Rapp, J. Aerosol Sci. **31**, 1367 (2000).